Long Lifetime and High-Fidelity Quantum Memory of Photonic Polarization Qubit by Lifting Zeeman Degeneracy

Zhongxiao Xu, Yuelong Wu, Long Tian, Lirong Chen, Zhiying Zhang, Zhihui Yan, Shujing Li, Hai Wang,*
Changde Xie, and Kunchi Peng

The State Key Laboratory of Quantum Optics and Quantum Optics Devices, Institute of Opto-Electronics, Shanxi University, Taiyuan, 030006, People's Republic of China

(Received 7 August 2013; published 10 December 2013)

Long-lived and high-fidelity memory for a photonic polarization qubit (PPQ) is crucial for constructing quantum networks. We present a millisecond storage system based on electromagnetically induced transparency, in which a moderate magnetic field is applied on a cold-atom cloud to lift Zeeman degeneracy and, thus, the PPQ states are stored as two magnetic-field-insensitive spin waves. Especially, the influence of magnetic-field-sensitive spin waves on the storage performances is almost totally avoided. The measured average fidelities of the polarization states are 98.6% at 200 μs and 78.4% at 4.5 ms, respectively.

DOI: 10.1103/PhysRevLett.111.240503 PACS numbers: 03.67.Hk, 37.10.−x, 42.50.Ex, 42.50.Gy

Quantum memories [1] for single-photon polarization qubits are crucial for establishing entanglement between two remote atomic ensembles in quantum repeater protocols [2–7]. In recent years, many physical processes, such as spontaneous Raman emission (SRE) [8,9], electromagnetically induced transparency (EIT) [10–12], atomic-frequency combs (AFC) [13,14], off-resonant Raman interaction [15], and others [16,17] have been exploited to store quantum states of light. The absorptive EIT and emissive SRE processes in cold atoms provide promising storage schemes, based on which high retrieval efficiencies [18,19] and long lifetimes [8,9,11,12] have been demonstrated. The SRE process is an elementary step in the Duan-Lukin-Cirac-Zoller (DLCZ) protocol [2], which can create a single photon correlated with one collective excitation. By detecting a single photon which could be emitted from either of the two ensembles, a heralded entanglement between two ensembles can be established [2,7]. However, with the DLCZ protocol the probability p of generating an excitation in two ensembles has to be very low ($p \ll 1$) for suppressing the errors resulting from unwanted multiple emissions [3,20]. But as $p \rightarrow 0$, the influences of the experimental imperfections, such as stray light scattering and detector dark counts on the fidelity of entanglement will be more conspicuous [21]. To overcome this drawback, alternative approaches based on single-photon sources [3] and polarization-entangled photon pairs (see Sec. III C in Ref. [4]) in combination with quantum memories have been proposed, in which the absorptive memory schemes such as EIT [10] or AFC [14] are used for storing single-photon qubits. Since single photons are provided by ideal or quasi-ideal single-photon sources, the multiple emission errors existing in the DLCZ protocol are naturally eliminated [3–5] in these protocols. To complete the protocols based on single-photon detections [2,3], the phase stability over a long distance is required and the requirement is difficult to be realized experimentally [4,5,7]. However, the protocol proposed in Ref. [4] relies on the two-photon detections to construct the long-distance entanglement, and thus relaxes the requirement for the phase stability [4,5]. To perform the two-photon detections, quantum storage of photonic polarization qubits (PPQs) is needed [4]. Quantum memories [1] capable of storing arbitrary polarization states of light have been implemented in a number of different media, including single atoms [22], cold atoms [20,23–27], warm vapors [28,29], and rare-earth-ion-doped crystals [30–32]. Toward realizing the quantum repeater, several experiments of EIT-based storage of a PPQ have been implemented in the quantum region [20,23,24]. In the experiments of Refs. [20,23], single-photon polarization qubits are split into vertical and horizontal components and then stored in two atomic systems, respectively, placed at two spatially separated arms of an interferometer, and the achieved storage lifetime is several microseconds. Another EIT-based storage experiment of PPQ is realized in a Bose-Einstein condensation [24], in which the memory qubit is preserved in two atomic magnetic-field-sensitive (MFS) coherences $m = 0 \leftrightarrow m' = \pm 1$, and the residual magnetic field is actively compensated to reduce the decoherence. The measured polarization fidelities in Ref. [24] are ~0.95 for the storage period of 2 μs and ~0.75 for 470 μs, respectively, which is the longest storage lifetime of PPQ obtained with an EIT-based scheme, so far. To increase the storage lifetime PPQs should be encoded in atomic coherences associated with magnetic-field-insensitive (MFI) transitions, which have been utilized in the DLCZ-type experiments [26,27]. In Ref. [26], Kuzmich's group creates a memory qubit whose logical states are preserved in two spin waves (SWs) associated with the MFI coherences $m = \pm 1 \leftrightarrow m' = \mp 1$ of two overlapped atomic ensembles confined in a 1D optical lattice. Although the experiment demonstrates the violation of Bell's equality for the storage time of 3 ms, the unwanted MFS SWs are also produced during the creation of the qubit memory, which leads to the retrieval efficiency decreasing promptly after the storage time of 100 μs [9,26]. Besides, due to the interference between the clock SW ($m = 0 \leftrightarrow m' = 0$) and the MFI SWs, the higher entanglement appears only at the periodical interval of $T = nt$, where $t = 0.54$ ms and $n = 1, 2, 3 \ldots$ [26]. Also, the same group realizes the quantum memory with a lifetime of 100 ms by encoding qubit states in two spatially distinct SWs associated with the $m = 0 \leftrightarrow m' = 0$ clock coherence and applying a magic-valued magnetic field to eliminate the lattice-induced dephasing [27]. However, because of the spatial splitting of the SW qubit states, some extra steps, such as the interferometric stability [7] and spatially matching the two SW modes, are required.

Until now, the EIT-based scheme of storing PPQs as MFI SWs has not been implemented. Here, we present an effective long lifetime and high-fidelity EIT-based storage experiment for PPQs. By applying a moderate magnetic field on a cold ^{87}Rb atomic cloud, only two pairs of MFI transitions appear respectively in two EIT systems existing within a cold atomic cloud, which will be used for storing the PPQ states. At the same time, all MFS transitions are removed outside of the EIT systems when the degeneracy of Zeeman sublevels is lifted. Thus, the influences of MFS coherences on the storage are eliminated and the performances of the qubit memory are significantly improved.

The involved levels of ^{87}Rb atoms and the experimental setup are shown in Figs. 1(a)–1(c), respectively,

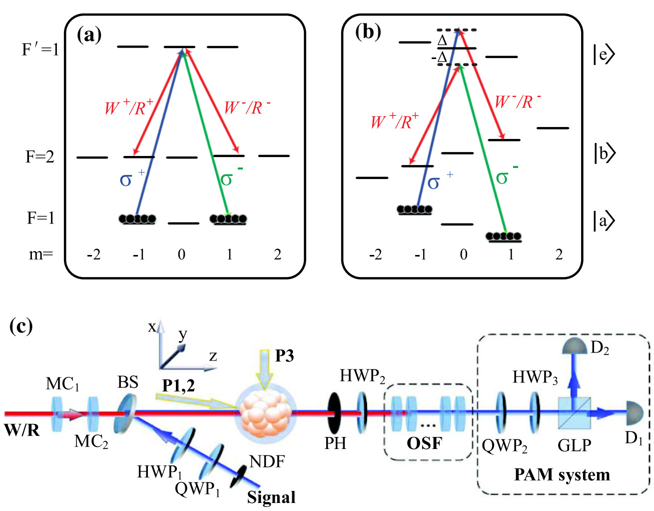

FIG. 1 (color online). Overview of the experiment. (a) and (b) The atomic level schemes of ^{87}Rb with a weak ($B_0 = 0.59$ G) and a moderate ($B_0 = 13.5$ G) magnetic field, respectively. σ^+ and σ^- are right-and left-polarized signal light fields, respectively. (c) The experimental setup. Acronyms are defined in the text except for neutral density filters (NDF) and the Glan-laser polarizer (GLP).

where $|a\rangle = |5^2S_{1/2}, F = 1\rangle$, $|b\rangle = |5^2S_{1/2}, F = 2\rangle$, and $|e\rangle = |5^2P_{1/2}, F' = 1\rangle$. All of the atoms are in an incoherent mixture of the $m = \pm 1$ states (m denotes the magnetic quantum number). The signal and writing-reading light fields are tuned to transitions $|a\rangle \leftrightarrow |e\rangle$ and $|b\rangle \leftrightarrow |e\rangle$, respectively; their frequency difference is ω_{ab}, which matches the resonance of the two-photon transition $|a\rangle \leftrightarrow |b\rangle$ at the case of Zeeman degeneracy. For suppressing the dephasing effect resulting from atomic motion, we make the signal and writing-reading light beams collinearly go through the cold-atom cloud along the z direction. Such a collinear configuration was first proposed and demonstrated by Zhao *et al.* [8] in the DLCZ-type experiment, in which they achieved the storage lifetime of ~1 ms for single photons with a fixed polarization. In the presented experiment, the input signal-light field may be set in an arbitrary polarization state, which can be regarded as the superposition of the right-circularly (σ^+) and left-circularly (σ^-) polarized components. Since the quantum axis is defined by applying a bias magnetic field B_0 along the z direction, the $\sigma^\pm$-polarized components of a signal photon couple to $|a_m\rangle \leftrightarrow |e_{m+1}\rangle$ and $|a_m\rangle \leftrightarrow |e_{m-1}\rangle$ transitions, respectively. The writing-reading light field is vertically polarized and its $\sigma^\pm$-polarized components ($W^\pm/R^\pm$) drive the $|b_m\rangle \leftrightarrow |e_{m+1}\rangle$ and $|b_m\rangle \leftrightarrow |e_{m-1}\rangle$ transitions, respectively. In previous EIT-based storage of PPQs [20,24], the typical value of the magnetic fields used to define the quantization axis is about several hundreds of mG. When such a weak field is applied on the ^{87}Rb atomic ensembles, the degeneracy of the Zeeman sublevels of $F = 1$ and 2 ground states is not lifted [see Fig. 1(a)]. In this case, for the σ^+-(σ^--) polarized component, the EIT occurs in the four-level tripod system [33] formed by $|a_{m=-1}\rangle - |b_{m=-1}\rangle - |e_{m=0}\rangle - |b_{m=1}\rangle$ ($|a_{m=1}\rangle - |b_{m=1}\rangle - |e_{m=0}\rangle - |b_{m=-1}\rangle$). By switching off the writing beam, the σ^+-(σ^--) polarized component of the input signal is transferred into SWs $S_{-1,1}$ ($S_{1,-1}$) and $S_{-1,-1}$ ($S_{1,1}$), and stored in the cloud of cold atoms, where $S_{-1,1}$ ($S_{1,-1}$) is associated with the MFI coherence $|a_{m=-1}\rangle \leftrightarrow |b_{m=1}\rangle$ ($|a_{m=1}\rangle \leftrightarrow |b_{m=-1}\rangle$), while $S_{1,1}$ ($S_{-1,-1}$) is associated with the MFS coherence $|a_{m=1}\rangle \leftrightarrow |b_{m=1}\rangle$ ($|a_{m=-1}\rangle \leftrightarrow |b_{m=-1}\rangle$). In our experiment, the degeneracy of Zeeman sublevels is obviously lifted [see Fig. 1(b)] by applying a moderate magnetic field along the z direction. The frequency of the MFI $|a_{m=1}\rangle \leftrightarrow |b_{m=-1}\rangle$ ($|a_{m=-1}\rangle \leftrightarrow |b_{m=1}\rangle$) transition still matches ω_{ab}, while the frequency of the MFS $|a_{m=1}\rangle \leftrightarrow |b_{m=1}\rangle$ ($|a_{m=-1}\rangle \leftrightarrow |b_{m=-1}\rangle$) transition becomes mismatching ω_{ab}. Therefore, the four-level tripod EIT system will change to the three-level Λ-type EIT system formed by $|a_{m=-1}\rangle - |e_{m=0}\rangle - |b_{m=1}\rangle$ ($|a_{m=1}\rangle - |e_{m=0}\rangle - |b_{m=-1}\rangle$) and the σ^+-or σ^--polarized component of signal photons will be only transferred into the MFI SW $S_{-1,1}$ or $S_{1,-1}$. By using dark-state polariton concepts [10,33,34], we obtain the retrieval efficiencies of $\sigma^\pm$-polarized signal photons

$$R_e^{\pm}(t) = R_{e0}e^{-(t/\tau_1^z)}e^{-(t/\tau_D)} = R_{e0}e^{-(t/\tau_1)} \quad (1)$$

for the case of the lifting-Zeeman degeneracy [see Eqs. (S13)–(S14) in the Supplemental Material [35]], and

$$R_e^{\pm}(t) = \frac{1}{4}R_{e0}\left| e^{(-t/2\tau_1^z)-i\omega_{\mp1,\pm1}t} + e^{(-t/2\tau_{\mp1,\mp1}^z)-i\omega_{\mp1,\mp1}t}\right|^2 e^{-(t/\tau_D)} \quad (2)$$

for the case of the Zeeman degeneracy [see Eq. (S11) in the Supplemental Material [35]], respectively, where $\omega_{m,m'}$ is the Larmor frequency of the SWs $\hat{S}_{m,m'}(z,t)$, $\tau_1 = \tau_D\tau_1^z/(\tau_D+\tau_1^z)$, τ_D is the lifetime limited by the atomic motion [7,8], $\tau_1^z = \tau_{1,-1}^z = \tau_{-1,1}^z$ is the lifetime of the MFI SWs $S_{1,-1}$ or $S_{-1,1}$, $\tau_{-1,-1}^z$ ($\tau_{1,1}^z$) is the lifetime of the MFS SW $S_{-1,-1}(S_{1,1})$; the lifetimes $\tau_{m,m'}^z$ are limited by inhomogeneous Zeeman broadening [7,9]. We theoretically evaluate the retrieval efficiencies for both cases of lifting and nonlifting Zeeman degeneracy according to Eqs. (1) and (2), respectively. For our system with a cloud of cold atoms of ~200 μK temperature and a signal light beam of ~1 mm diameter, we calculated $\tau_D \approx 3.3$ ms [see Ref. [8] or Eq. (S4) in the Supplemental Material [35]]. The measured magnetic field gradients B' in our magneto-optical trap are ~10 and 35 mG/cm for a weak (0.59 G) and a moderate (13.5 G) field, respectively, and the calculated lifetimes are $\{\tau_1^z = \tau_{1,-1}^z = \tau_{-1,1}^z \approx 16.2$ ms, $\tau_{-1,-1}^z = \tau_{1,1}^z \approx 32\ \mu\text{s}\}$, and $\tau_1^z = \tau_{1,-1}^z = \tau_{-1,1}^z \approx 4.6$ ms for the fields of 0.59 and 13.5 G, respectively [see Ref. [9] or Eq. (S5) in the Supplemental Material [35]]. Substituting above data into Eqs. (1) and (2), it is shown that the retrieval efficiency of the σ^+-(σ^--) polarized signal photons for the lifting-Zeeman-degenerate case is about 4 times that for the Zeeman-degenerate case at storage times longer than ~100 μs. The physical reason is that the partial optical signals are transferred into the MFS SW $S_{1,1}$ ($S_{-1,-1}$), which reduces to a very low level within 100 μs.

As shown in Fig. 1(c), the input signal and writing-reading light beams are combined by a polarization-insensitive beam splitter (BS). Before arriving at the BS, the signal beam goes through neutral density filters, a quarter-wave plate (QWP1) and a half-wave plate (HWP1). By adjusting the QWP1 and HWP1, the polarization state of the signal light can be arbitrarily set. The optical mode cleaners $MC_{1,2}$ (see the Supplemental Material [35]) are used to filter the incoherent components of the writing-reading laser pulses. After reaching the BS, the signal and the writing-reading beams collinearly propagate through the cold atoms along the z direction. The writing-reading beam and the stray light are blocked by a pinhole (PH) and optical spectral filters (OSFs), i.e., Fabry-Perot cavities [35], while the retrieval signal photons go through a half-wave plate HWP_2 and then enter into a polarization analyzing and measuring (PAM) system. The HWP_2 is used to compensate the relative phase between the σ^+-polarized and σ^--polarized retrieval photons and PAM is utilized to perform the polarization analyzing and measuring of the retrieved photons [35]. In the PAM system, D_1 and D_2 denote photodiode detectors for measuring retrieval efficiencies in Fig. 2 or single-photon detectors for polarization fidelity measurements in Fig. 3 and Table I.

The cold ^{87}Rb atomic cloud is collected by the magneto-optical trap and then a Sisyphus cooling is performed. After the 0.7-ms Sisyphus cooling, the bias magnetic field B_0 is switched on for a duration of 0.5 ms to reach a stabilization value (0.59 or 13.5 G) and then the pumping lasers $P1, 2, 3$ and the writing laser are turned on. Keeping the optical pumping for 18 μs, most of the atoms have been prepared into the states $|a_{m=1}\rangle$ or $|a_{m=-1}\rangle$ with equal populations, and the measured optical depth for the transition $|a_{m=\pm1}\rangle \leftrightarrow |e_{m=0}\rangle$ is ~4. After the pumping, i.e., at the time $t = 0$, the signal pulses (with a pulse length of 100 ns) are switched on and stored into the cloud of cold atoms by dynamic EIT (see the Supplemental Material [35]). Waiting for a period t, the stored SWs are retrieved by switching on the reading beam and are detected within a window of ~100 ns.

First, we perform the storage and retrieval experiments of the σ^+-(σ^--) polarized signal light with its input peak power of 25 μW. The measured retrieval efficiencies of $\sigma^{\pm}$-polarized signal fields as the function of storage time at $B_0 = 0.59$ G are shown in Figs. 2(a) and 2(b) (red circle dots), respectively. We can see that they fast drop to a very low level around ~80 μs, which is because the MFS SWs are washed out at times longer than ~80 μs. The solid green lines II and II' are fits to the experimental data based

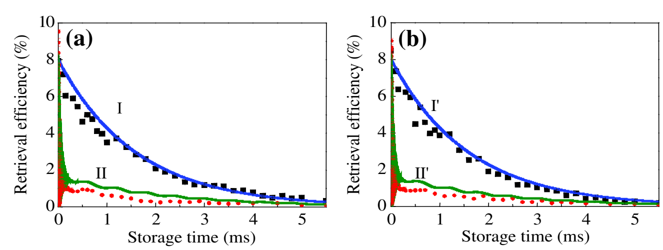

FIG. 2 (color online). Measured retrieval efficiencies as the function of the storage time t for the σ^+-polarized (a) and σ^--polarized (b) signal fields. Black square and red circular points are the experimental data obtained for $B_0 = 13.5$ and $B_0 = 0.59$ G, respectively. The blue solid lines I in (a) and I' in (b) are the fittings to the experimental data (black square points) according to $R_e^{\pm}(t) = R_{e0}e^{-t/\tau_1}$, respectively, which yields $R_{e0} = 8.3\%$, $\tau_1 = 1.6$ ms. The fitting result of 1.6 ms is close to the calculated value $\tau_1 = \tau_D\tau_1^z/(\tau_D+\tau_1^z) \approx 1.9$ ms, where $\tau_D \approx 3.3$ ms and $\tau_1^z \approx 4.6$ ms are the evaluated results in the text. The green lines II in (a) and II' in (b) are the fittings to the experimental data (red circular points) according to theoretical models in which the imperfect atomic preparation has been taken into account (see the Supplemental Material [35]).

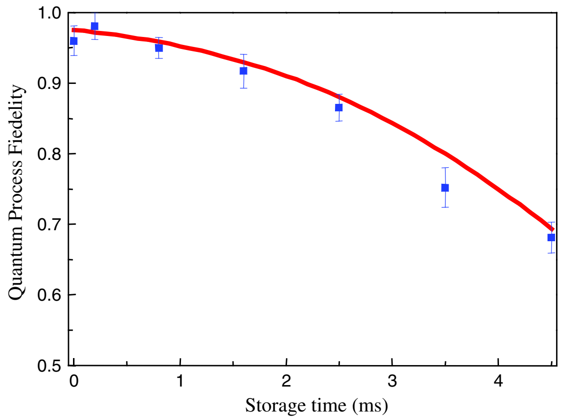

FIG. 3 (color online). Quantum process fidelity as the function of storage time t. The data are fitted by Eq. (3), with the measured total detection efficiency $\eta_d \approx 0.19$ and background noise $N = 2.2 \times 10^{-4}$. The retrieval efficiencies $R_e^{\pm}(t) = 0.083e^{-t/1.6}$ are obtained from both fitting curves I and I' in Fig. 2. The fitting yields the e^{-1} dephasing time of $\sigma_\gamma = 14$ ms.

on theoretical models. In the models, the influences of imperfect atomic preparation have been taken into account (see the Supplemental Material [35]), and thus the fittings are in good agreement with the measured results. The black square dots in Figs. 2(a) and 2(b) are the measured retrieval efficiencies of $\sigma^{\pm}$-polarized signal fields at $B_0 = 13.5$ G, respectively. The solid blue lines I and I' are the fits to the experimental data based on Eq. (1), with a storage lifetime of $\tau_1 = 1.6$ ms and the retrieval efficiency $R_{e0} = 8.3\%$ at $t = 0$. Comparing the curves I (I') and II (II'), we find that the measured retrieval efficiencies with $B_0 = 13.5$ G is ~4 times that with $B_0 = 0.59$ G at times longer than ~80 μs, which is in perfect agreement with the theoretical prediction mentioned above. At $B_0 = 13.5$ G, the two retrieval efficiencies for the σ^+-and σ^--polarized signal photons are symmetric and the storages are long lived, which provides promise for achieving a high-fidelity and long lifetime storage of a PPQ.

Subsequently, we perform the storage and retrieval of the PPQ with $B_0 = 13.5$ G. The input signal pulse is decreased to the single-photon level (i.e., the mean photon number $\bar{n} = 1$) by using the neutral density filters. $\bar{n}$ is determined by detecting the probability per pulse at the case without the cold atomic cloud and considering the total detection efficiency of $\eta_d \approx 19\%$ (see the Supplemental Material [35]). To characterize the quality of the qubit memory, we perform experiments of storage and retrieval for four input polarization states $|H\rangle$, $|V\rangle$, $|D\rangle$, and $|R\rangle$, respectively. By analyzing the retrieval photon in three mutually unbiased bases $|H\rangle - |V\rangle|$, $|R\rangle - |L\rangle$, and $|D\rangle - |A\rangle$, we reconstruct the density matrix $\rho_{\rm out}$ of the retrieved single photons by means of the quantum state tomography [35,36], where H, V, R, L, D, and A denote horizontal, vertical, right circular, left circular, diagonal (45°), and antidiagonal (−45°) polarizations, respectively. The fidelity of the quantum state is defined as the overlap of the density matrix $\rho_{\rm out}$ with the ideal input state $|\psi_i\rangle$:$F_{\rm st} = \langle\psi_i|\rho_{\rm out}|\psi_i\rangle$. The fidelities of the four input states at several different storage times are listed in Table I. The measured average fidelity is 98.6% at 200 μs and decreases to 78.4% at 4.5 ms.

Alternatively, the storage of PPQ can be characterized by the quantum process matrix $\mathcal{X}$ [37]. After reconstructing the matrix $\mathcal{X}$ (see the Supplemental Material [35]), we obtain quantum-process fidelity $F_{\rm process}$, which is defined as

$$F_{\rm process} = {\rm Tr}\left(\sqrt{\sqrt{\chi}\chi^{\rm ideal}\sqrt{\chi}}\right)^2,$$

with $\chi_{0,0}^{\rm ideal} = 1$ [35]. The function of $F_{\rm process}$ as the storage time is shown in Fig. 3, from which we can see that $F_{\rm process}$ decreases with the storage time. We attribute the decrease to the following two factors. First, since the retrieval efficiency exponentially reduces with the storage time, the background noise gradually becomes a main contribution to the single-photon-counting events which make the polarization fidelity reduce. On the other hand, the dephasing between the two spin waves $S_{1,-1}$ and $S_{-1,1}$, induced by the temporal fluctuations of the magnetic field in the z direction will decrease the retrieval fidelity also. Considering all the above-mentioned factors, a formula used for evaluating the quantum process fidelity is deduced (see the Supplemental Material [35]),

TABLE I. Quantum state fidelities of the four input polarization states for several storage times. $F_{{\rm st}(X)}$ are the measured state fidelities, respectively, for four different input polarized states of photons ($X = H, V, D, R$) without any background noise subtraction; $F_{\rm ava} = (F_{{\rm st}(H)} + F_{{\rm st}(V)} + F_{{\rm st}(D)} + F_{{\rm st}(R)})/4$ is the average fidelity; t is the storage time. The errors are obtained by Monte Carlo simulation which takes into account the statistical uncertainty of photon counts.

t(μs)	$F_{{\rm st}(H)}$ (%)	$F_{{\rm st}(V)}$ (%)	$F_{{\rm st}(D)}$ (%)	$F_{{\rm st}(R)}$ (%)	$F_{\rm ava}$ (%)
2	96.7 ± 1.2	98 ± 1.1	97.7 ± 1.1	98.7 ± 0.85	97.8 ± 1.06
200	98.3 ± 1.2	98.1 ± 1.1	98.1 ± 1.1	99.8 ± 0.19	98.6 ± 0.89
800	95.5 ± 1.5	97 ± 1.3	96 ± 1.3	97.6 ± 1.2	96.5 ± 1.33
1600	94.1 ± 1.5	94.5 ± 1.7	94.6 ± 1.6	96.4 ± 1.3	94.9 ± 1.5
2500	90.7 ± 2.0	91 ± 2.0	89 ± 2.0	91.9 ± 2.0	90.7 ± 2
3500	85.7 ± 2.3	82.6 ± 2.6	87.7 ± 2.3	84 ± 2.6	84.0 ± 2.45
4500	82 ± 2.8	72 ± 3.2	79.4 ± 2.9	80 ± 2.9	78.4 ± 2.95

$$F_{\text{process}} \approx \frac{[1+\gamma(t)]\eta_d R_e(t) + N}{2[\eta_d R_e(t) + 2N]}, \quad (3)$$

where $\gamma(t) = \exp[-t^2/\sigma_\gamma^2]$ is the dephasing factor, η_d is the total detection efficiency, and $R_e(t)$ is the retrieval efficiency. N corresponds to the relative background noise. The solid line is the fitting to the data of the quantum-process fidelity according to (3), which is in good agreement with the measured results. The fitting yields the e^{-1} dephasing time of $\sigma_\gamma = 14$ ms, which corresponds to the magnetic-field temporal fluctuations of $\sigma_B \approx 3$ mG [35]. If an active compensation technology is utilized to reduce the magnetic-field fluctuations to $\sigma_B \approx 0.3$ mG, the dephasing time of ~100 ms is expected. Besides, after the writing process is finished, if we decrease the magnetic field from ~13.5 to 3.23 G during storage, the used coherences $|a_{m=\pm1}\rangle \leftrightarrow |b_{m=\mp1}\rangle$ will become the perfect first-order magnetically insensitive coherences [11], and thus the dephasing time will further increase.

In summary, we have proposed and experimentally demonstrated an EIT-based quantum storage approach for PPQs with long lifetime and high fidelity. By lifting Zeeman degeneracy, the MFS transitions are removed from EIT systems and the signal photons are only mapped on two MFI SWs. In this case, the bad influences of MFS SWs on the storage ability are eliminated and thus the storage performance is significantly improved. Within the storage time of less than 4.5 ms, the measured average fidelity is higher than the threshold of 78% for the violation of the Bell inequality [38,39]. The demonstrated approach is robust because only a cold atomic cloud is applied in the system and thus the interference between the two spatially separated modes is not needed. If the cloud of cold atoms is placed in an optical cavity [19,40] the retrieval efficiency can be further improved. The demonstrated qubit memory approach can be utilized to store the polarization-entangled photon pairs [19] or a single-photon polarization qubit [24] for realizing long-distance quantum communication [2,4,7] and implementing distributed quantum computing [41]. Especially, the achieved millisecond storage approach is robust and then can be applied in multiplexed devices for realizing long-distance entanglement distribution over ~1000 km [42].

We acknowledge funding support from the 973 Program (2010CB923103) and the National Natural Science Foundation of China (Grants No. 10874106, No. 11274211, and No. 61121064).

*Corresponding author.
wanghai@sxu.edu.cn

[1] A. I. Lvovsky, B. C. Sanders, and W. Tittel, Nat. Photonics 3, 706 (2009).
[2] L. M. Duan, M. D. Lukin, J. I. Cirac, and P. Zoller, Nature (London) 414, 413 (2001).
[3] N. Sangouard, C. Simon, J. Minář, H. Zbinden, H. de Riedmatten, and N. Gisin, Phys. Rev. A 76, 050301(R) (2007).
[4] Z. B. Chen, B. Zhao, Y. A. Chen, J. Schmiedmayer, and J. W. Pan, Phys. Rev. A 76, 022329 (2007).
[5] N. Sangouard, C. Simon, B. Zhao, Y. Chen, H. de Riedmatten, J. W. Pan, and N. Gisin, Phys. Rev. A 77, 062301 (2008).
[6] C. Simon, H. De Riedmatten, M. Afzelius, N. Sangouard, H. Zbinden, and N. Gisin, Phys. Rev. Lett. 98, 190503 (2007).
[7] N. Sangouard, C. Simon, H. De Riedmatten, and N. Gisin, Rev. Mod. Phys. 83, 33 (2011).
[8] B. Zhao, Y. A. Chen, X. H. Bao, T. Strassel, C. S. Chuu, X-M. Jin, J. Schmiedmayer, Z. S. Yuan, S. Chen, and J. W. Pan, Nat. Phys. 5, 95 (2009).
[9] R. Zhao, Y. O. Dudin, S. D. Jenkins, C. J. Campbell, D. N. Matsukevich, T. A. B. Kennedy, and A. Kuzmich, Nat. Phys. 5, 100 (2009).
[10] M. Fleischhauer and M. D. Lukin, Phys. Rev. Lett. 84, 5094 (2000).
[11] U. Schnorrberger, J. D. Thompson, S. Trotzky, R. Pugatch, N. Davidson, S. Kuhr, and I. Bloch, Phys. Rev. Lett. 103, 033003 (2009).
[12] R. Zhang, S. R. Garner, and L. V. Hau, Phys. Rev. Lett. 103, 233602 (2009).
[13] E. Saglamyurek, N. Sinclair, J. Jin, J. A. Slater, D. Oblak, F. Bussières, M. George, R. Ricken, W. Sohler, and W. Tittel, Phys. Rev. Lett. 108, 083602 (2012).
[14] C. Clausen, I. Usmani, F. Bussières, N. Sangouard, M. Afzelius, H. De Riedmatten, and N. Gisin, Nature (London) 469, 508 (2011).
[15] K. F. Reim, P. Michelberger, K. C. Lee, J. Nunn, N. K. Langford, and I. A. Walmsley, Phys. Rev. Lett. 107, 053603 (2011).
[16] M. Hosseini, B. M. Sparkes, G. Campbell, P. K. Lam, and B. C. Buchler, Nat. Commun. 2, 174 (2011).
[17] B. Julsgaard, J. Sherson, J. I. Cirac, J. Fiuráek, and E. S. Polzik, Nature (London) 432, 482 (2004).
[18] Y. H. Chen, M. J. Lee, I. C. Wang, S. W. Du, Y. F. Chen, Y. C. Chen, and I. A. Yu, Phys. Rev. Lett. 110, 083601 (2013).
[19] X. H. Bao, A. Reingruber, P. Dietrich, J. Rui, A. Dück, T. Strassel, L. Li, N. L. Liu, B. Zhao, and J. W. Pan, Nat. Phys. 8, 517 (2012).
[20] K. S. Choi, H. Deng, J. Laurat, and H. J. Kimble, Nature (London) 452, 67 (2008).
[21] S. Chen, Y. Chen, T. Strasse, Z. S. Yuan, B. Zhao, J. Schmiedmayer, and J. W. Pan, Phys. Rev. Lett. 97, 173004 (2006)
[22] P. S. Holger, N. Christian, R. Andreas, U. Manuel, F. Eden, R. Stephan, and G. Rempe, Nature (London) 473, 190 (2011).
[23] H. Zhang, X-M. Jin, J. Yang, H. N. Dai, S. J. Yang, T. M. Zhao, J. Rui, Y. He, X. Jiang, F. Yang, G. S. Pan, Z. S. Yuan, Y. J. Deng, Z. B. Chen, X. H. Bao, S. Chen, B. Zhao, and J. W. Pan, Nat. Photonics 5, 628 (2011).
[24] M. Lettner, M. Mücke, S. Riedl, C. Vo, C. Hahn, S. Baur, J. Bochmann, S. Ritter, S. Dürr, and G. Rempe, Phys. Rev. Lett. 106, 210503 (2011).
[25] H. Tanji, S. Ghosh, J. Simon, B. Bloom, and V. Vuletić, Phys. Rev. Lett. 103, 043601 (2009).

[26] Y. O. Dudin, S. D. Jenkins, R. Zhao, D. N. Matsukevich, A. Kuzmich, and T. A. B. Kennedy, Phys. Rev. Lett. **103**, 020505 (2009).
[27] Y. O. Dudin, A. G. Radnaev, R. Zhao, J. Z. Blumoff, T. A. B. Kennedy, and A. Kuzmich, Phys. Rev. Lett. **105**, 260502 (2010).
[28] Y. W. Cho and Y. H. Kim, Opt. Express **18**, 25 786 (2010).
[29] D. G. England, P. S. Michelberger, T. F. M. Champion, K. F. Reim, K. C. Lee, M. R. Sprague, X-M Jin, N. K. Langford, W. S. Kolthammer, J. Nunn, and I. A. Walmsley, J. Phys. B **45**, 124008 (2012).
[30] M. Gündoğan, P. M. Ledingham, A. Almasi, M. Cristiani, and H. De Riedmatten, Phys. Rev. Lett. **108**, 190504 (2012).
[31] Z. Q. Zhou, W. B. Lin, M. Yang, C. F. Li, and G. C. Guo, Phys. Rev. Lett. **108**, 190505 (2012).
[32] C. Clausen, F. Bussières, M. Afzelius, and N. Gisin, Phys. Rev. Lett. **108**, 190503 (2012).
[33] H. Wang, S. J. Li, Z. X. Xu, X. B. Zhao, L. J. Zhang, J. H. Li, Y. L. Wu., C. D. Xie., K. C. Peng, and M. Xiao, Phys. Rev. A **83**, 043815 (2011).
[34] A. Joshi and M. Xiao, Phys. Rev. A **71**, 041801(R) (2005)
[35] See Supplemental Material at http://link.aps.org/supplemental/10.1103/PhysRevLett.111.240503 for experimental details and calculations of retrieval efficiencies and polarization fidelity.
[36] D. F. V. James, P. G. Kwiat, W. J. Munro, and A. G. White, Phys. Rev. A **64**, 052312 (2001).
[37] J. L. O'Brien, G. J. Pryde, A. Gilchrist, D. F. V. James, N. K. Langford, T. C. Ralph, and A. G. White, Phys. Rev. Lett. **93**, 080502 (2004).
[38] H. N. Dai, H. Zhang, S. J. Yang, T. M. Zhao, J. Rui, Y. J. Deng, L. Li, N. L. Liu, S. Chen, X. H. Bao, X-M. Jin, B. Zhao, and J. W. Pan, Phys. Rev. Lett. **108**, 210501 (2012).
[39] M. Aspelmeyer, H. R. Böhm, T. Gyatso, T. Jennewein, R. Kaltenbaek, M. Lindenthal, G. Molina-Terriza, A. Poppe, K. Resch, M. Taraba, R. Ursin, P. Walther, and A. Zeilinger, Science **301**, 621 (2003).
[40] M. Sabooni, Q. Li, S. Kröll, and L. Rippe, Phys. Rev. Lett. **110**, 133604 (2013).
[41] J. W. Pan, Z. B. Chen, C. Y. Lu, H. Weinfurter, A. Zeilinger, and M. Żukowski, Rev. Mod. Phys. **84**, 777 (2012).
[42] O. A. Collins, S. D. Jenkins, A. Kuzmich, and T. A. B. Kennedy, Phys. Rev. Lett. **98**, 060502 (2007).